Equilibrium Denaturation of Recombinant Human FK Binding Protein in Urea†

D. A. Egan, T. M. Logan, H. Liang, E. Matayoshi, S. W. Fesik, and T. F. Holzman*

Drug Design and Delivery, Pharmaceutical Products Division, Abbott Laboratories, Abbott Park, Illinois 60064

Received October 6, 1992; Revised Manuscript Received December 8, 1992

ABSTRACT: The equilibrium folding behavior of recombinant human FK-binding protein, a peptidyl-prolyl *cis–trans*-isomerase, was examined by urea-induced denaturation using probes of protein structure including intrinsic tryptophan fluorescence, second-derivative UV absorbance, CD, and NMR. All optical probes of protein structure indicate that FKBP is capable of folding reversibly. The second-derivative UV absorbance and CD probes of the structure exhibited urea denaturation transitions at ~4.3 M urea. The fluorescence of the single protein tryptophan is quenched in the folded state. During the unfolding–folding transition, the unquenching of tryptophan fluorescence occurs at a slightly lower urea concentration (3.9 M urea) than the changes observed for the other optical probes of folding. These probes of structure demonstrate little dependence on protein concentration in the range of 0.2–~3 mg/mL across the urea-induced denaturation transition. The reversibility of the unfolding–folding transition was confirmed from two-dimensional $^{15}N/^{1}H$ heteronuclear single-quantum coherence (HSQC) spectra of [U-^{15}N]FKBP. In addition, the native–denatured transitions for 57 individual amino acids were determined from an analysis of these spectra acquired at different urea concentrations. Analysis of the transitions for all clearly observable HSQC cross peaks for residues distributed throughout the protein and comparison to the optical folding transitions, indicate that FKBP global folding is consistent with a two-state process. Although direct measurement of FKBP catalytic activity in urea was complex, enzyme activity was observed up to the beginning of the FKBP urea-denaturation transition. Taken together, these data provide a base line set of conditions, at urea concentrations below the folding transition of FKBP, under which it is possible to utilize FKBP as a tool in the study of urea-induced proline-dependent protein/peptide folding.

As originally shown by Anfinsen for ribonuclease in vitro (1961), the amino acid sequence of a protein contains sufficient information to determine the protein tertiary structure. Thus, the protein native state reflects the sum of interactions between its constituent amino acids and bulk solvent. These interactions give rise to a folded linear amino acid sequence which is maintained in a native-state conformation by a dynamic balance of noncovalent interactions (hydrophobic, ionic, and hydrogen bonding) and covalent disulfide linkages. The mechanisms of and processes occurring in protein folding are of central interest to the study of protein structure. The pathways for protein folding in vitro can be generally characterized by the occurrence of three events: a hydrophobic collapse, the appearance of a secondary structural framework, and the eventual formation of intermediate or final-state intramolecular disulfide-linked species through covalent adhesion steps (Kim & Baldwin, 1990). Analyses of structural events associated with protein folding in vitro have focused on the archetypal *framework* and *modular assembly* "working models" (Kim & Baldwin, 1982). Irrespective of the type of working model for protein folding, evidence indicates that certain slow folding/unfolding reactions in vitro involve proline isomerization (Brandts et al., 1975). Conversion between X-Pro isomers is typically observed during the terminal steps of folding after secondary structure is established in vitro (Kim & Baldwin, 1990, and references cited therein). A number of direct tests for the involvement of proline isomerization have been devised including isomer-specific proteolysis (Lin & Brandts, 1979, 1985) and site-directed mutagenesis (Kim & Baldwin, 1990, and references cited therein). A recent approach to testing the involvement of proline isomerization in protein folding has been the use of the peptidyl-prolyl isomerase[1] (PPIase) cyclophilin (Fischer et al., 1984). For example, cyclophilin has been shown to accelerate the slow proline-related final folding step in ribonuclease (Fischer & Bang, 1985) and to accelerate the refolding of type II and type III collagens (Bachinger, 1987; Davis et al., 1989). However, in the case of calbindin, which exists in two folded forms differing in the cis–trans isomerization state of a single X-Pro amide (Kordel et al., 1990), cyclophilin did not accelerate isomer interconversion. This observation suggests that conformational and steric restrictions prevent the folded form of the protein from acting as a substrate for cyclophilin.

The potential use of PPIases as tools for studying the folding of a particular target protein/peptide in vitro makes it desirable to determine a priori the folding behavior of the isomerase using one or more methods of differential inactivation (Citri, 1973) which typically employ thermal or chemical denaturation/renaturation strategies (Ghelis & Yon, 1982a; Kim & Baldwin, 1982; Pace, 1988). In this paper, we examine the folding behavior of a peptidyl-prolyl isomerase under conditions of urea-induced denaturation. We have focused on the cloned human-derived FKBP (Maki et al., 1990) for these studies because it has a number of desirable properties. FK binding protein (FKBP) is a recently described member of the family of peptidyl-prolyl isomerases (Siekierka et al., 1989, 1990;

† This research was supported in part by a grant from the National Institutes of Health (GM45351).

* Address correspondence to this author at Protein Biochemistry, D-46Y, AP-10-1, Discovery Research, Abbott Laboratories, Abbott Park, IL 60064.

[1] The enzyme catalyzes the cis–trans-isomerization of peptide bonds and is, therefore, categorized under the EC 5.2 class as a *cis–trans*-isomerase. The enzyme has also been termed a 'rotamase'. Abbreviations: DTT, dithiothreitol; EDTA, ethylenediaminetetraacetic acid; Hepes, *N*-(2-hydroxyethyl)piperazine-*N*′-2-ethanesulfonic acid; HSQC, heteronuclear single-quantum coherence spectroscopy; rhFKBP, recombinant human FK binding protein; SDS–PAGE, sodium dodecyl sulfate–polyacrylamide gel electrophoresis.

0006-2960/93/0432-1920$04.00/0

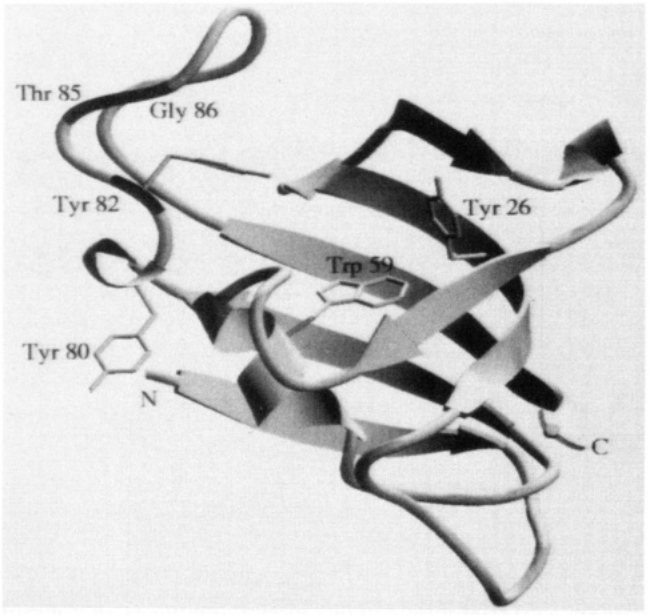

FIGURE 1: Ribbon diagram of the three-dimensional structure of FKBP showing the locations of protein Trp 59, Tyr 26, Tyr 80, Tyr 82, Thr 85, and Gly 86.

Harding et al., 1989). It has been shown to catalyze the cis–trans isomerization of X-Pro bonds in certain artificial substrates (Siekierka et al., 1989, 1990; Harding et al., 1989) and, like cyclophilin, is of interest in transplantation research and protein folding in vivo (DeFranco, 1991; Enosawa et al., 1991; Flanagan et al., 1991; Liu et al., 1991; Gething & Sambrook, 1992). It is structurally distinct from cyclophilin, but like cyclophilin is also widely distributed. It is smaller than cyclophilin and has only one potentially reactive sulfhydryl group. In addition, it has recently been expressed at extremely high levels in *Escherichia coli* (~300 mg of purified enzyme/L of cells, Edalji et al., 1992) so that preparation of gram quantities of the protein are practical. Detailed information on the secondary and tertiary structure of FKBP has recently been obtained (Michnick et al., 1991; Van Duyne et al., 1991). The protein has 107 residues (M_W = 11 819) and is composed of five strands of anti-parallel β-sheet and a single segment of α-helix (Figure 1). FKBP possesses a single Trp residue (59) and three Tyr residues (26, 80, 82). These aromatic residues along with several Phe residues (46, 48, 99) compose an aromatic pocket comprising the binding region for FK-506 (Van Duyne et al., 1991) and the related immunosuppressant, ascomycin (Petros et al., 1991).

MATERIALS AND METHODS

Sample Preparation. Recombinant-derived FKBP was expressed in *Escherichia coli*, grown on minimal media containing either NH_4Cl or $^{15}NH_4Cl$ using a variant of the CKS–FKBP fusion technique recently described (Edalji et al., 1992). FKBP was purified from *E. coli* cell lysates using isolation protocols and conditions identical to those recently described for the recombinant human PPIase cyclophilin (Holzman et al., 1991). All samples of the purified FKBP used for these studies exhibited single N-termini and single bands on SDS–PAGE. Urea (ultrapure) was purchased from Schwarz/Mann. Final urea concentrations were determined by refractive index (Pace, 1988). Protein concentrations were estimated using an ϵ^{278} = 9927 M^{-1} cm^{-1}, calculated from the amino acid composition (Gill & Von Hippel, 1989). Purified FKBP, typically at 2–3 mg/mL, was concentrated to ~10 mg/mL with a Centriprep 10 (Amicon, Inc.) and exchanged with buffer A (75 mM sodium phosphate, 25 mM glycine, 1.0 mM DTT, 0.04% sodium azide, pH 7.2), stored under argon; the added glycine functioned as a cyanide scavenger (Pace, 1988). The concentrated, exchange protein was then diluted 10–20-fold into various combinations of buffer A and buffer A with 10 M urea. The protein samples were allowed to equilibrate in the final urea concentrations (specified in the figures) for at least 1 h before optical spectrscopic measurements were made. Samples for NMR spectroscopy were prepared using [U-^{15}N]FKBP as described above at a final concentration of 1 mM in 0.5 mL. FKBP assays were performed as described in Figure 7 legend using the method of Kofron et al. (1991) to enhance the initial levels of the cis form of the FKBP substrate, *N*-succinyl-Ala-Leu-Pro-Phe-*p*-nitroanilide.

UV Absorbance, Fluorescence, and Circular Dichroism. All measurements were performed at 25.0 °C unless otherwise noted. Second-derivative UV absorbance measurements were made with a Hewlett Packard HP 8452A diode array spectrophotometer with 1-nm resolution. Sample absorbance was measured from 190 to 510 nm. The second-derivative UV signals associated with tyrosine exposure during folding in urea were calculated as previously described (Servillo et al., 1982; Rangone et al., 1984; Holzman et al., 1986). Fluorescence measurements were made with a Shimadzu RF-5000 spectrofluorimeter in a fashion similar to that reported previously (Holzman et al., 1990) using 5-mm path length cuvettes. The excitation wavelength was 294 nm with a 3-nm bandwidth. Emission spectra were acquired from 300 to 500 nm with a 3-nm bandwidth. All fluorescence data presented are technical spectra plotted as relative fluorescence and were obtained with identical instrument settings. Previous analysis has shown no effects of urea on the intrinsic fluorescence of the standard, *N*-acetyltryptophanamide (Holzman et al., 1990). For analysis of protein concentration dependence of fluorescence, samples were corrected for inner-filter effects using the estimation described by Lackowicz (1983). Circular dichroism measurements were made on a Jasco J-600 spectropolarimeter using 1-mm path length cuvettes. Spectra were acquired from 350 to 205 nm with a 1-nm bandwidth at a scan rate of 0.83 nm/s. Two scans were averaged for each sample.

NMR Spectroscopy. All NMR measurements were performed at 25 °C on a Bruker AMX500 NMR spectrometer operating at a 500 MHz proton frequency. Two-dimensional $^{15}N/^{1}H$ correlation experiments (Bodenhausen & Ruben, 1980) were recorded with 320 and 2048 complex points in t_1 and t_2, respectively. The total acquisition time for each experiment was 4 h. The H_2O signal was suppressed using the method of Messerle et al. (1989). To account for changes in probe tuning upon addition of urea, the probe was retuned and the 90° pulse widths were determined for each sample.

The data were apodized by a 90° shifted sine bell in both the t_1 and t_2 dimensions, and the frequency domain data were baseline corrected with a fifth-order polynomial in both dimensions. To improve the quality of the baseline correction in the ^{1}H dimension, only points downfield of the urea signal (5.8 ppm) were used to determine the baseline. Volume integrals were obtained for the assigned residues of unliganded FKBP (Rosen et al., 1991) and for an additional 30 noise "peaks" scattered around the spectral region of native FKBP. For each 2D spectrum in the urea denaturation curve, an average noise level was calculated, and this value was subtracted from the volume of each FKBP cross peak. The noise-corrected cross peak volumes for each urea concentration

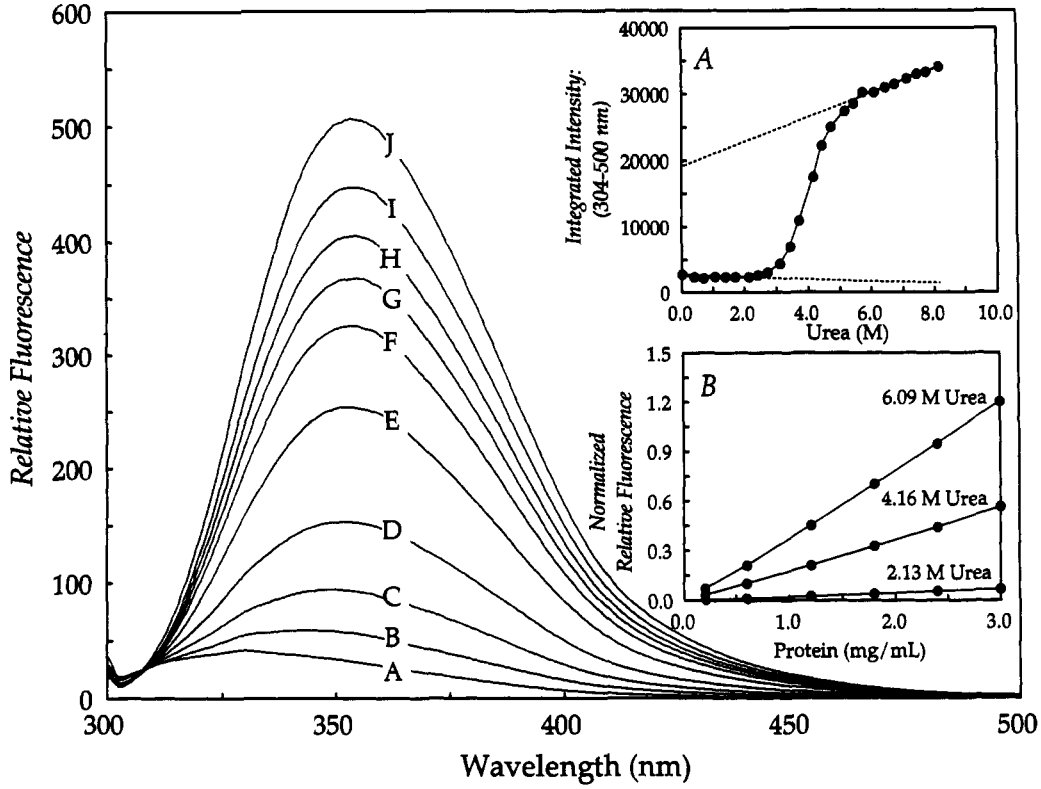

FIGURE 2: Urea-induced denaturation of FKBP measured by intrinsic tryptophan fluorescence. All spectra were obtained with identical instrument settings in both the main figure and inset A. Samples contained 50 μM FKBP, 75 mM phosphate buffer, 25 mM glycine, 1 mM DTT, pH 7.2, and varying concentrations of urea. The technical fluorescence spectra were measured at 25.0 °C using λ_{excit} = 294 nm and 3 nm excitation and emission slit widths. Spectra A–J were obtained in urea concentrations of 0.0, 3.1, 3.4, 3.7, 4.1, 4.4, 4.7, 5.1, 6.1, 7.1 M, respectively. Inset A: Equilibrium denaturation curve of FKBP based on integrated emission intensities from 304 to 500 nm. The dashed lines represent linear fits to the respective pre- and postdenaturation transition baselines; the data below 2.4 M urea and above 5.8 M urea were used to compute these baselines. Inset B: A plot of fluorescence intensity at 350 nm versus protein concentration at the pre-, mid-, and posttransition points for urea concentration. The fluorescence intensities were taken from the digitized spectral data and are corrected for inner-filter effects using the estimation of Lakowicz (1983).

were normalized to the cross peak volumes calculated for the sample in the absence of urea. Estimates for the urea denaturation midpoints of individual amides on the FKBP backbone were calculated from the normalized volume data using methods previously described for optical spectral probes (Pace, 1988).

RESULTS AND DISCUSSION

Spectral Probes of Urea-Induced Equilibrium Denaturation of FKBP. The effects of urea on the unfolding of rhFKBP as monitored by intrinsic fluorescence of the single protein tryptophan (Figure 1) is presented in Figure 2. The urea denaturation profiles for exactly the same samples, sequentially analyzed for changes in second-derivative UV and CD signals, are presented in Figures 3 and 4. In Figure 2, it is evident that in the native state the intrinsic fluorescence of the single-protein tryptophan residue is quenched relative to the unfolded state. The indole side chain extends out from the short helical segment, encompassing residues 56–64, and faces into the binding pocket which can be occupied by the immunosuppressant FK-506 (Van Duyne et al., 1991) and ascomycin (Petros et al., 1991) (Figure 1). In the presence of bound ligand, it forms the "floor" of the binding pocket and interacts with piperidine ring in FK-506 (Van Duyne et al., 1991) and ascomycin (Petros et al., 1991). Upon unfolding, the integrated intrinsic fluorescence of the protein tryptophan undergoes a ~12-fold increase (from 0 to 8 M urea) consistent with a strongly quenched native state (Figure 2 curves A–J and inset A). The pre- and postdenaturation fluorescence intensity transitions were linear but exhibited nonzero slopes

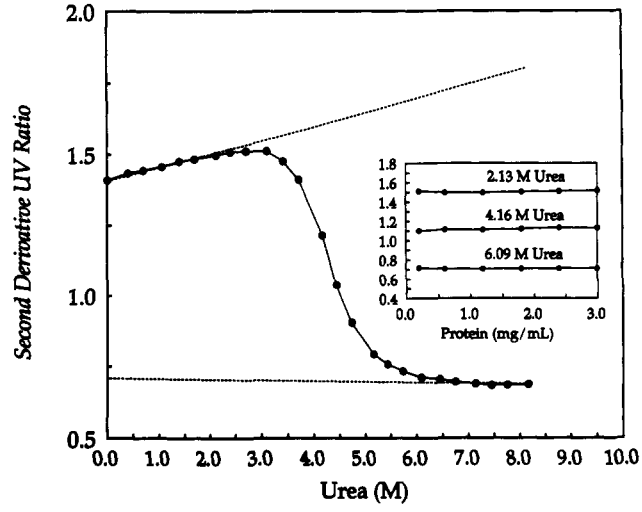

FIGURE 3: Urea-induced denaturation of FKBP measured by second-derivative UV peak ratio. Absorbance spectra were acquired and second-derivative ratios were calculated as described under Materials and Methods. Samples contained 50 μM FKBP, 75 mM phosphate buffer, 25 mM glycine, and 1 mM DTT, pH 7.2, and varying concentrations of urea were scanned after equilibrium at 25.0 °C. The dashed lines represent linear fits to the respective pre- and postdenaturation transition baselines; the data points below 2.2 M urea and above 6.5 M urea were used to compute these baselines. Inset: A plot of second-derivative ratio versus protein concentration at the pre-, mid-, and posttransition points for urea concentration.

(Figure 2, inset A). In order to distinguish intramolecular events from intermolecular events, the effect of protein

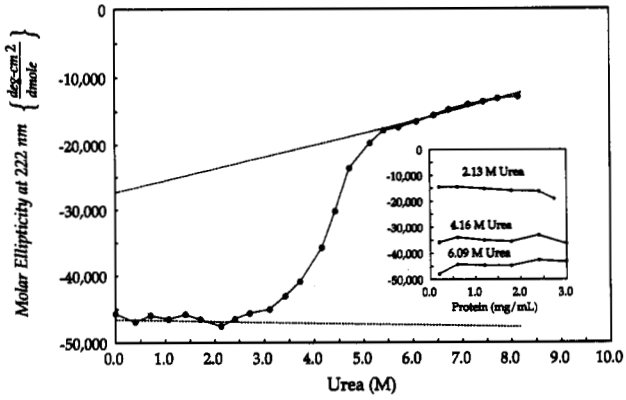

FIGURE 4: Urea-induced denaturation of FKBP measured by protein CD signal at 222 nm. Spectra were acquired as described under Materials and Methods. Samples contained 50 μM FKBP, 75 mM phosphate buffer, 25 mM glycine, and 1 mM DTT, pH 7.2, and varying concentrations of urea were scanned after equilibration. The dashed lines represent linear fits to the respective pre- and postdenaturation transition baselines; the data below 2.6 M urea and above 6.0 M urea were used to compute these baselines. Inset: A plot of molar ellipticity versus protein concentration at the pre-, mid-, and posttransition points for urea-induced denaturation.

concentration on the intrinsic fluorescence was examined across a ~15-fold range at the midpoint and on either side of the fluorescence intensity transition (Figure 2, inset B). The tryptophan fluorescence intensity exhibited a linear dependence on protein concentration; the λ_{max} of emission was independent of protein concentration over the same concentration range (data not shown). Therefore, the changes in fluorescence quenching are independent of protein concentration under the conditions examined and appear to be exclusively a function of intramolecular conformational events.

Previous studies have shown both UV difference spectroscopy and UV second-derivative spectroscopy to be useful indicators of protein conformation (Donovan, 1969, 1973; Servillo et al., 1982; Rangone et al., 1984). For proteins with Tyr–Trp ratios of 2:1 or higher, second-derivative spectroscopy is a particularly useful method for observing changes in protein Tyr exposure or burial in solvents of various polarities (Rangone et al., 1984). The ratio of Tyr–Trp (3:1) in FKBP suggested that it would be possible to use this method to follow exposure of protein Tyr residues to bulk solvent during urea denaturation. The extent of Tyr "burial" is reflected in the ratio of the peak–trough values from the second-derivative spectrum of protein absorbance, i.e., the peak–trough difference between the maximum at 295 nm and the minimum at 290 nm divided by the peak–trough difference between the maximum at 287 nm and the minimum at 283 nm. In Figure 3, this second-derivative UV ratio for FKBP is plotted as a function of urea concentration. It is evident that exposure to urea induces a change in this ratio consistent with exposure of protein Tyr residues to solvent during unfolding. Like the protein tryptophan fluorescence, the second-derivative UV ratio exhibited a denaturation transition with linear pre- and posttransition baselines but nonzero slopes (Figure 3). The effects of protein concentration on the second-derivative signal are presented in the inset to Figure 3. The second-derivative UV ratio was analyzed at urea concentrations on either side of the denaturation transition and at the transition midpoint. The ratios are essentially constant for protein concentrations over a ~15-fold range (up to 3.0 mg/mL) and indicate there is no significant protein concentration dependence of the exposure of Tyr residues across the folding transition. Thus, like the protein Trp fluorescence, the protein second-derivative absorbance must be sensitive solely to intramolecular conformational events during equilibrium denaturation. The fluorescence and second-derivative absorbance transitions indicate that unfolding exposes protein tyrosines to bulk solvent and disrupts native-state quenching of the protein Trp indole side chain. The three-dimensional structure of FKBP (Figure 1) and the FK-506/FKBP complex (Van Duyne et al., 1991) indicate Tyr residues at positions 26 and 82, contributed by (respectively) the fourth strand of the β-sheet and the loop connecting the second and the third strands of the β-sheet, are integrally involved in forming part of the enzyme immunosuppressant binding pocket. Thus, urea-induced exposure of protein Tyr residues would appear to reflect disruption of side-chain interactions within the ligand binding pocket, and it is, therefore, likely that the reduction in Trp fluorescence quenching also coincides with disruption of the binding pocket.

While fluorescence and UV spectroscopies can be useful for examining solvent or ligand-induced alterations in protein 3° structure, CD spectroscopy is particularly useful for analyzing the effects of conformational events on protein 2° structure. Alterations in 2° structure can often be detected through changes in the specific CD bands associated with α-helix, β-sheet, and random coil. The 2° structure of FKBP has been shown to be almost entirely composed of β-sheet (Figure 1). This type of secondary structure typically has two prominent CD transitions: a broad minimum near ~217 nm and a maximum near ~195 nm. The single short helical segment in the protein (Figure 1) would typically exhibit a broad doublet minimum between ~205 and ~230 nm and a maximum at ~192 nm. Since accurate CD measurements are very difficult to obtain in high concentrations of urea or guanidine at wavelengths below approximately 210 nm due to the very high background absorbancies of the denaturants themselves, the effect of urea on FKBP structure was measured at 222 nm. This wavelength was within the typical minima observed for α-helix and β-sheet and functioned to monitor combined changes in both types of secondary structure. The effect of urea on the molar ellipticity of the protein is presented in Figure 4. The figure inset contains the same protein concentration dependence analysis as presented for the effect of urea on protein fluorescence and second-derivative UV signals. The urea-induced CD transition in protein 2° structure occurs in the same urea concentration range as the 3° structural probes of second-derivative UV signal and Trp fluorescence quenching (Figures 2 and 3). Like both probes of 3° structure, the protein 2° structure CD denaturation transition exhibited linear pre- and posttransition baselines but nonzero slopes (Figure 4). Although there is a slight dependence of the CD signal on protein concentration at 2.13 M urea (Figure 4, inset) and there is some variation in the CD signals for the 4.16 and 6.09 M urea concentrations (Figure 4, inset), the overall effects of a ~15-fold change in protein concentration on the CD signals across the urea-induced CD denaturation transition are small.

With the availability of appropriately labeled protein samples, one of the most useful tools for probing protein conformation is heteronuclear multidimensional NMR. Figure 5A depicts a 2D $^{15}N/^{1}H$ heteronuclear single-quantum coherence (HSQC) spectrum (Bodenhausen & Ruben, 1980) of [U-^{15}N]FKBP obtained in the absence of urea. As typically observed for folded proteins, the chemical environment is unique for many of the backbone amides, generating a dispersion in the chemical shifts of individual amide resonances. On addition of urea, the resonances corresponding to native FKBP decrease in intensity and a second set of resonances appear corresponding to unfolded protein (Figure 5B). At

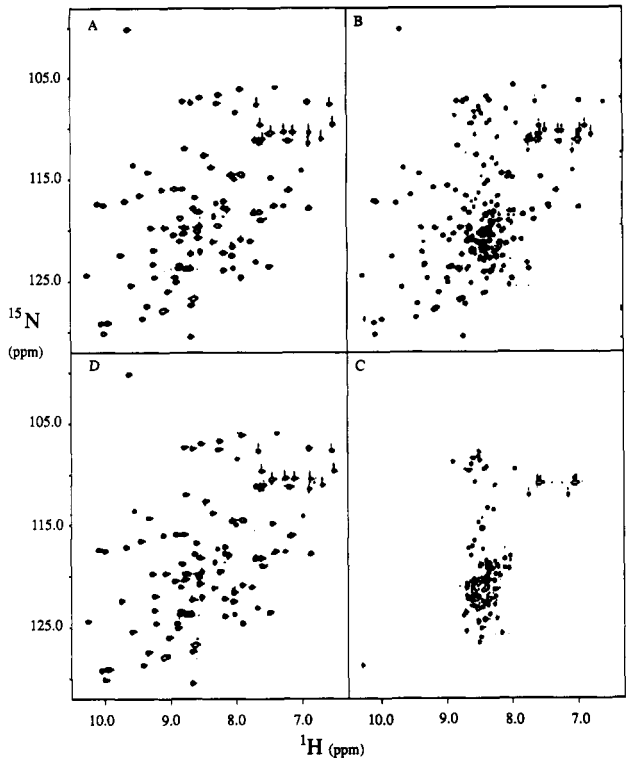

FIGURE 5: 2D ^{15}N/^{1}H heteronuclear single-quantum coherence (HSQC) spectra of [U-^{15}N]FKBP obtained in the presence and absence of various concentrations of urea. All samples were prepared in buffer A (10% D_2O), pH 7.2. Panel A: Protein in buffer alone. Panel B: Protein in buffer with 4.2 M urea. Panel C: Protein in buffer with 8.3 M urea. Panel D: Protein from unfolded conditions of 8.3 M urea of panel C after exhaustive dialysis into buffer A alone.

urea concentrations greater than 6.0 M, only resonances of unfolded FKBP are observed in the spectrum (Figure 5C). The chemical shift dispersion and the high sensitivity of the HSQC experiment allow accurate integrations of the ^{15}N/^{1}H cross peaks as a function of urea concentration. Denaturation profiles for 57 of the 100 possible residues (Pro residues do not have amide protons and are not observed in this experiment) distributed over the entire FKBP backbone were obtained in this manner. Complete denaturation profiles for some residues could not be determined due to overlap with other signals. Figure 6 shows the normalized mean integrated cross peak volumes of ^{15}N/^{1}H resonances for these 57 residues. The data form a denaturation profile consisting of linear and essentially zero-slope pre- and posttransition baselines. All of the integrated residues exhibit unfolding in concert and are distributed throughout the sheet, helix, and random 2° structural elements of the protein. Several cross peaks of native FKBP exhibited increased intensity upon addition of urea (Figure 6). These residues, Tyr 82, Thr 85, and Gly 86, are all located in a large loop between the second and third strands of the β-sheet (Figure 1). As seen in Figure 6, these three residues exhibit increases in cross peak intensity of as much as 2-fold upon addition of urea and then remain at constant intensity until denaturing. In previous NMR studies of FKBP, Rosen et al. (1991) observed less intensity for the ^{15}N/^{1}H cross peaks of Tyr 82 and Gly 86 compared to the other residues in an HSQC spectrum. The intensity difference was attributed to the exchange broadening of these signals, possibly associated with ring-flips of a nearby aromatic residue. The increased intensity observed in our NMR experiments suggests a shift in the equilibrium between the different species or a change in the rate of exchange between different species upon addition of urea in such a fashion that the exchange broadening is diminished.

Urea-Induced Denaturation Is Reversible. Although irreversible protein denaturation phenomena are measurable, they are typically difficult to interpret in terms of meaningful *reversible* folding mechanisms, even if the irreversible process is considered to consist of a series discrete kinetically controlled metastable states, each of which is *mostly* reversible (Ghelis & Yon, 1983b). Thus, establishing the reversibility of denaturant-induced unfolding becomes paramount for any subsequent analyses of structural or conformational contributions to folding. The reversibility of FKBP folding was analyzed by optical spectroscopy (data not shown) and 2D NMR (Figure 5). To test reversibility by optical spectroscopic probes of protein structure, samples of FKBP in buffer alone (folded) and in 8.0 M urea (unfolded) were diluted to an intermediate urea concentration of 4.0 M along with samples simply diluted into buffer alone and 8.0 M urea. The final protein concentration was 50 μM FKBP in 75 mM phosphate buffer, 25 mM glycine, and 1 mM DTT, pH 7.2, 25.0 °C, at the specified urea concentration. After equilibration (4 h), changes were recorded in sample intrinsic protein tryptophan fluorescence spectra, second-derivative UV spectra, and CD spectra. The resulting spectra demonstrated that proceeding from either the folded state or the unfolded state to the intermediate urea concentration produced equivalent spectral characteristics. The similarity of the spectra for the folded → partially unfolded and unfolded → partially folded transitions is consistent with a reversible process. Although the optical probes of folding appear reversible, NMR techniques can provide a much more detailed and global view of the reversibility of folding and the return of 2° and 3° structural signatures of the protein to native state conditions. The reversibility of folding in urea was examined by NMR in the 2D ^{15}N/^{1}H HSQC spectra of native FKBP (Figure 5A) and FKBP refolded from 8.0 M urea (Figure 5D). Comparison of these spectra, which are highly sensitive to differences in structure, shows that the renatured FKBP is identical to native FKBP. In addition to spectroscopic tests of folding, NMR ligand binding analyses and enzyme assays confirm the recovery of the native state (data not shown).

Urea-Induced Denaturation of FKBP Is a Global Two-State Process. In order to establish the existence of a simple two-state folding process, it is useful to demonstrate both the coincidence of probes of folding and the absence of aggregated forms through the unfolding transition. As indicated above, optical spectroscopic probes of FKBP protein conformation gave little indication of intermolecular events which might coincide with the equilibrium unfolding/folding transitions. Similarly, line broadening, which would result from a decrease in the protein rotational rate during unfolding, was not observed in either 1D proton NMR analyses of FKBP across the folding transition (data not shown) or 2D ^{15}N/^{1}H HSQC experiments. Thus, these data support the conclusion that the unfolding of FKBP does not lead to the formation of partially folded aggregated states under partially denaturing conditions. The fit of certain of the spectroscopic probes of structure to a simple two-state model for folding is examined in Figure 7. For a protein obeying a two-state folding model, all probes of structure should exhibit coincident changes across the range of denaturant concentrations used to unfold the protein. In the main panel, after correction for pre- and posttransition baselines (Pace, 1988), the data for the optical and NMR probes of structure are plotted as fraction denatured versus urea concentration. In inset A, the apparent equilibrium

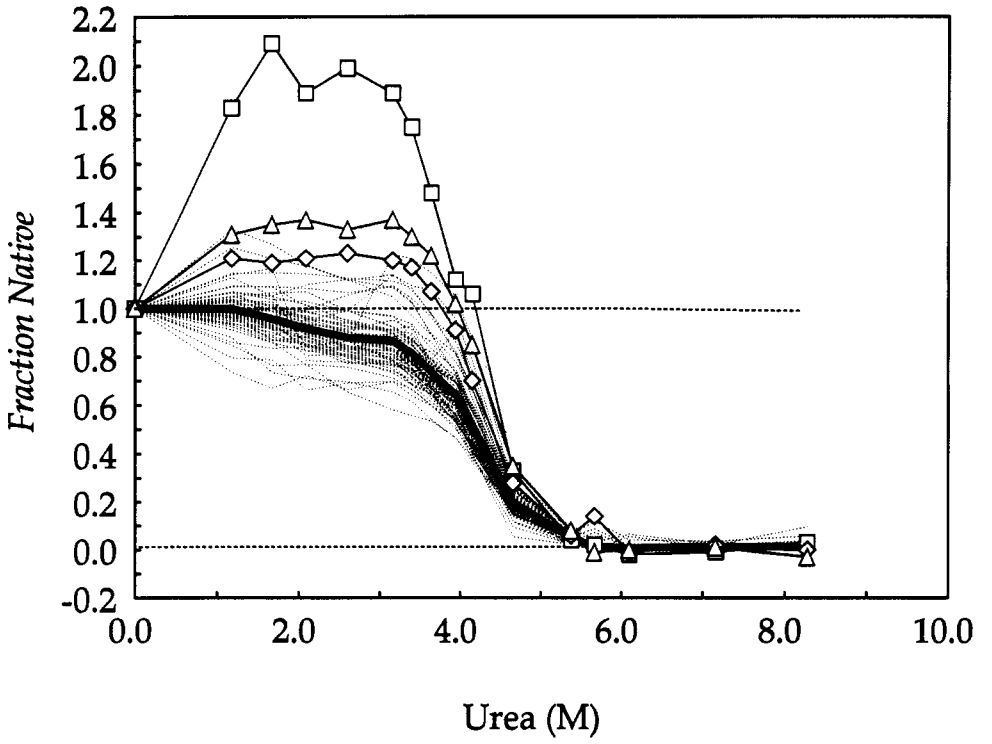

FIGURE 6: Urea-induced denaturation of [U-^{15}N]FKBP measured by integration of 2D ^{15}N/^{1}H heteronuclear single-quantum coherence (HSQC) spectral cross peaks. Spectra were acquired as described under Materials and Methods. Samples contained 1.0 mM FKBP, 75 mM buffer, 25 mM glycine, and 1 mM DTT, pH 7.2, and varying concentrations of urea were analyzed after equilibration at 25.0 °C. Integrated cross peak volumes for all residues were normalized to volumes observed for the HSQC spectrum in the absence of urea. Solid thick line, normalized mean integrated volumes for 57 of 108 residues of FKBP which were spectrally well separated in the HSQC analyses and integrable across the entire urea denaturation transition, thin dashed lines are the traces for individual residues. The near-horizontal straight dashed lines represent linear fits to the respective pre- and postdenaturation transition baselines; the data below 2.0 M urea and above 5.8 M urea were used to compute these baselines. Open squares, normalized mean integrated area values for Thr 85; open triangles, normalized mean integrated area values for Gly 86; open diamonds, normalized mean integrated area values for Tyr 82.

constant for folding is plotted versus urea concentration to yield the apparent $\Delta G_{D,H_2O}$ on extrapolation to 0 M urea and the midpoint ($\Delta G_D = 0$) for the denaturation transition for each probe (Pace, 1988) (Figure 7, inset A legend). The UV, CD, and NMR probes of structure appear coincident (Figure 7, main panel); they give essentially identical urea concentrations for $\Delta G_D = 0$ and similar free energies of unfolding (Figure 7, inset A legend). However, the change in fluorescence quenching, measured using the same samples producing the UV and CD data, occurs at a lower urea concentration than the denaturation-related changes in second-derivative UV, CD, and NMR signals, but exhibits essentially the same free energy of unfolding (Figure 7, inset A legend).

Thus, the spectral probes of FKBP folding fall into two classes: those with coincident transitions (UV second-derivative, CD, and NMR) and the noncoincident tryptophan fluorescence quenching (Figure 7, main panel). If a protein has stable folding intermediates which are characterized by a macroscopic feature Y_i and concentration f_i, then the detected extent of unfolding is $f_{obs} = f_{den} + \Sigma_i f_i Z_i$, where $Z_i = (Y_i - Y_{den})/(Y_{den} - Y_{nat})$ (Tanford, 1968). This expression indicates the contribution of intermediates to the extent of unfolding, f_{obs}, is weighted by the Z_i value for the intermediate. For probes of structure which are related to the properties of the entire molecule, such as the CD or the "averaged" NMR signals, the value of Z_i for an intermediate will approximate the limit of unfolding of the entire molecule (Pace, 1988). Thus, to a first approximation, these probes of structure directly reflect conformation and can be used to observe the "global" folding of the protein and to aid in discerning the existence of stable "global" intermediates. For FKBP the unfolding/folding transitions observed by CD and NMR are essentially coincident; by these measures FKBP folding obeys a two-state process. The extent of tyrosine exposure, represented by the UV second-derivative signal, also appears to reflect "global" folding and is consistent with a two-state process. This is not surprising since the three Tyr residues are not localized to a single stretch of protein sequence or to a small, local, three-dimensional volume within the protein (Figure 1). Protein tryptophan fluorescence, by comparison, is generally dependent on the particular properties of a "local" microenvironment around the indole side chain. In FKBP, the single Trp faces into the hydrophobic protein "pocket" (Figure 1) and exhibits quenched fluorescence in the native state. The change in intrinsic fluorescence during folding occurs at a urea concentration only slightly lower than that observed for the probes of "global" structure (Figure 7, main panel). Based on the coincident folding behavior observed for the CD signal and the sizable fraction of protein residues observed by NMR, we conclude that these probes define a two-state global folding process for FKBP while the tryptophan fluorescence quenching likely represents a relatively local change in the microenvironment of the indole ring alone and/or the indole ring and intramolecular quenching group.

CONCLUSIONS

Analyses of the spectroscopic probes of FKBP denaturation in urea clearly indicate that the folding of FKBP is freely reversible. Upon return to native state, the protein is competent to bind ligands and is catalytically active. The probes of protein structure indicate that it is stable to urea concentrations below ~3 M and, thus, in principle, can be used in catalytic amounts to study the role of prolyl isomerization in protein folding reactions at or below this urea concentration. As a test of this

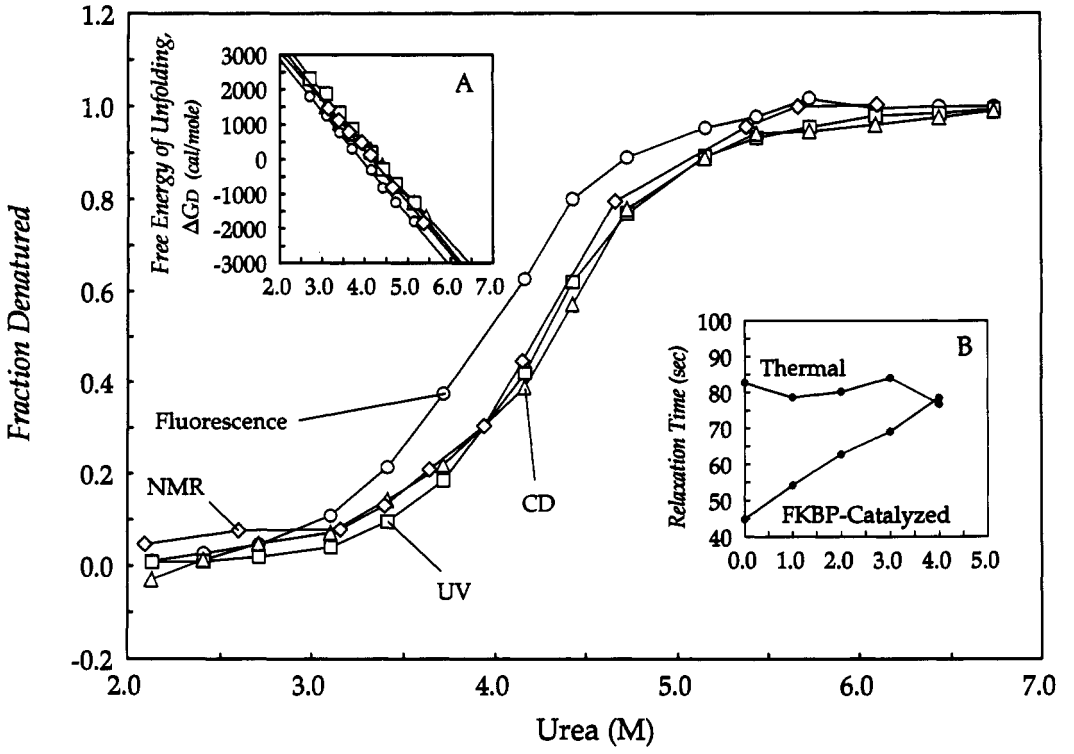

FIGURE 7: Fraction of denatured FKBP measured as a function of urea concentration. In the main panel, data are analyzed for a two-state (native – denatured) transition where fraction denatured = $(Y - Y_d)/(Y_d - Y_n)$, where Y_n, Y_d, and Y are the observable values for the native state, denatured state, and intermediate points in the transition. Fluorescence (circles), UV (squares), CD (triangles), and NMR (diamonds) data were taken from Figures 2–4, respectively, after correction for the calculated linear pre- and postdenaturation transition baselines depicted in the respective figures (Pace, 1988). Inset A: Linear approximation to the free energy of unfolding of FKBP calculated across the midpoints of the transitions depicted in the main panel as $-\ln(K_{app})RT$ (Pace, 1988). Where K_{app}, the apparent equilibrium constant for unfolding, was calculated as K_{app} = (fraction denatured/fraction native), R is the gas constant, and T is in K. The depicted least-square lines fitted to the free energy values for each spectra probe correspond to, respectively, fluorescence (intercept = 3.9 M urea at $\Delta G_{D=0}$, $\Delta G_{D(0.0\ M\ urea)}$ = 5.9 kcal/mol), UV second-derivative (intercept = 4.3 M urea at $\Delta G_{D=0}$, $\Delta G_{D(0.0\ M\ urea)}$ = 6.5 kcal/mol), CD (intercept = 4.3 M urea at $\Delta G_{D=0}$, $\Delta G_{D(0.0\ M\ urea)}$ = 5.8 kcal/mol), and NMR (intercept = 4.2 M urea at $\Delta G_{D=0}$, $\Delta G_{D(0.0\ M\ urea)}$ = 6.2 kcal/mol). Inset B: First-order rate constants, plotted as relaxation times, for cis–trans isomerization of the FKBP substrate, *N*-succinyl-ALPF-*p*NA, in the presence and absence of 8 nM FKBP and ~250 μM cis substrate, at 10 °C, pH 7.4. Total reaction times were typically under 5 min at this temperature. Prior to the initiation of each reaction, both FKBP and the coupling enzyme (chymotrypsin) were separately, and simultaneously, equilibrated for 1 h at each separate concentration of urea. Individual reaction mixtures were prepared by mixing appropriate volumes of stock solutions of FKBP and chymotrypsin at the specified urea concentration with an appropriate volume of reaction buffer. Each reaction buffer contained urea at the same final concentration as the separate, equilibrated samples of FKBP and chymotrypsin. Each reaction was initiated by the final addition of 10 μL of substrate in anhydrous trifluoroethanol/LiCl (Materials and Methods). Comparative measurements of FKBP acceleration of substrate cis–trans isomerization were only possible up to 4.0 M urea; at urea concentration above 4.0 M, the thermal rates observed for standard FKBP assay conditions were no longer a simple first-order process. Although initial chymotrypsin concentrations in the assay are typically greater than 200 μM (Kofron et al., 1991) and were here, as well, at initiation of the 1-h preassay incubation period, the actual chymotrypsin concentration present in solution at the time of assay is likely much lower due to losses from denaturation and/or autolysis.

process, we examined the activity of the enzyme in the improved (Kofron et al., 1991) peptidyl-prolyl isomerase assay (Fischer et al., 1984; Fischer & Bang, 1985) after equilibration in various urea concentrations (Figure 7, inset B). In this coupled assay, active FKBP will accelerate the isomerization of cis to trans substrate; only the trans substrate is cleaved by the coupling enzyme, chymotrypsin. Thus, the isomerase-catalyzed reaction will have a shorter relaxation time than the reaction in the absence of enzyme (Figure 7, inset B). Upon preincubation of assay components at the desired urea concentration, we found that ~4 M urea was the highest concentration which gave expected behavior for simple thermal cis → trans conversion of substrate (i.e., a good fit to a first-order process). At urea concentrations above 4 M, substrate cleavage kinetics significantly deviated from first-order (Figure 7, inset B legend). Because of these limitations in the spectrophotometric assay, which is based on the *p*-nitroanilide derivatives of peptide substrates, the data in Figure 7B likely under estimate the urea concentration range accessible to study with FKBP and other peptide–protein substrates. For example, it should be possible to maintain a constant "effective" level of folded (active) FKBP by varying FKBP concentrations in a folding reaction in *inverse* proportion to the extent of FKBP unfolding across its urea denaturation transition.

Given the different peptide sequence specificities displayed by cyclophilin and FKBP (Harrison & Stein, 1990), it would be useful to test both peptidy-prolyl isomerases in folding experiments where proline isomerization is believed to play a role. In addition to FKBP, we have also examined the folding behavior of human cyclophilin, produced by recombinant techniques (Holzman et al., 1991), using UV and fluorescence spectra probes of structure. We find that, in contrast to FKBP, recombinant human cyclophilin fails the reversibility test for these probes of structure and exhibits an irreversible kinetic loss of structure in both urea and guanidine (Holzman, unpublished observations). Therefore, because FKBP folds reversibly, it affords a more robust choice for analyzing the contributions of proline isomerization to protein folding.

ACKNOWLEDGMENT

The authors wish to thank Dr. Thomas Perun of Drug Design and Delivery and Dr. George Carter of Immunoscience

Research in Pharmaceutical Discovery Research at Abbott Laboratories for their support.

REFERENCES

Bachinger, H. P. (1987) *J. Biol. Chem. 262*, 17144–17148.

Bodenhausen, G., & Ruben, D. J. (1980) *Chem. Phys. Lett. 69*, 185–189.

Brandts, J. F., Halvorson, H. R. & Brennan, M. (1975) *Biochemistry 14*, 4953–4963.

Citri, N. (1973) *Adv. Enzymol. Relat. Areas Mol. Biol. 37*, 397–648.

Davis, J. M., Boswell, B. A., & Bachinger, H. P. (1989) *J. Biol. Chem. 264*, 8956–8962.

DeFranco, A. L. (1991) *Nature 352*, 754–755.

Donovan, J. W. (1969) *J. Biol. Chem. 244*, 1961–1967.

Donovan, J. W. (1973) *Methods Enzymol. 26*, 497–525.

Edalji, R., Pilot-Matias, T. J., Pratt, S. D., Egan, D. A., Severin, J. M., Gubbins, E. J., Petros, A. M., Fesik, S. W., Burres, N. S., & Holzman, T. F. (1992) *J. Protein Chem. 11*, 213–224.

Enosawa, S., Baird, M. A., & Heslop, B. F. (1991) *Transplantation 51*, 1318–1321.

Fischer, G., & Bang, H. (1985) *Biochim. Biophys. Acta 828*, 39–42.

Fischer, G., Bang, H., & Mech, C. (1984) *Biomed. Biochim. Acta 43*, 1101–1111.

Flanagan, M. W., Corthesy, B., Bram, R. J., & Crabtree, G. R. (1991) *Nature 352*, 803–807.

Gething, M. J., & Sambrook, J. (1992) *Nature 355*, 33–45.

Ghelis, C., & Yon, J. (1982a) *Protein Folding*, pp 225–330, Academic Press, New York.

Ghelis, C., & Yon, J. (1982b) *Protein Folding*, pp 27–33 and 340–373, Academic Press, New York.

Gill, S. C., & von Hippel, P. H. (1989) *Anal. Biochem. 182*, 319–326.

Harding, M. W., Galat, A., Uehling, D. E., & Schreiber, S. L. (1989) *Nature 341*, 758–760.

Harrison, R. K., & Stein, R. L. (1990) *Biochemistry 29*, 3813–3816.

Holzman, T. F., Brems, D. N., & Dougherty, J. J. (1986) *Biochemistry 25*, 6907–6917.

Holzman, T. F., Doughterty, J. J., Brems, D. N., & MacKenzie, N. E. (1990) *Biochemistry 29*, 1255–1261.

Holzman, T. F., Egan, D. A., Edalji, R., Simmer, R. L., Helfrich, R., Taylor, A., & Burres, N. S. (1991) *J. Biol. Chem. 266*, 2474–2479.

Kim, P. S., & Baldwin, R. L. (1982) *Annu. Rev. Biochem. 51*, 459–489.

Kim, P. S., & Baldwin, R. L. (1990) *Annu. Rev. Biochem. 59*, 631–660.

Kofron, J. L., Kuzmic, P., Kishore, V., Bonilla, E., & Rich, D. (1991) *Biochemistry 30*, 6127–6134.

Kordel, J., Drakenberg, T., Forsen, S., & Thulin, E. (1990) *FEBS Lett. 263*, 27–30.

Lackowicz, J. R. (1983) *Principles of Fluorescence Spectroscopy*, pp 43–49, Plenum Press, New York.

Lin, L. N., & Brandts, J. F. (1979) *Biochemistry 18*, 43–47.

Lin, L. N., Brandts, J. F. (1985) *Biochemistry 24*, 6533–6538.

Liu, J., Farmer, J. D., Lane, W. S., Friedman, J., Weissman, I., & Schreiber, S. L. (1991) *Cell 66*, 807–815.

Maki, N., Sekiguchi, F., Nishimaki, J., Miwa, K., Hayano, T., Takahashi, N., & Suzuki, M. (1990) *Proc. Natl. Acad. Sci. U.S.A. 87*, 5440–5443.

Messerle, B. A., Wider, G., Otting, G., Weber, C., & Wuthrich, K. (1989) *J. Magn. Res. 85*, 608–613.

Michnick, S. W., Rosen, M. K., Wandless, T. J., Karplus, M., & Schreiber, S. L. (1991) *Science 252*, 836–839.

Pace, C. N. (1988) *Methods Enzymol. 131*, 266–282.

Petros, A. M., Gampe, R. T., Gemmecker, G., Neri, P., Holzman, T. F., Edalji, R. Hochlowski, J., Jackson, M., McAlpine, J., Luly, J. R., Pilot-Matias, T., Pratt, S., & Fesik, S. W. (1991) *J. Med. Chem. 34*, 2925–2928.

Rangone, R., Colonna, G., Balestrieri, C., Servillo, L., & Gaetano, I. (1984) *Biochemistry 23*, 1871–1875.

Rosen, M. K., Michnick, S. W., Karplus, M., & Schreiber, S. L. (1991) *Biochemistry 30*, 4774–4789.

Servillo, L., Colonna, G., Balestrieri, C., Rangone, R., & Gaetano, I. (1982) *Anal. Biochem. 126*, 251–257.

Siekierka, J. J., Hung, S. H. Y., Poe, M., Lin, C. S., & Sigal, N. H. (1989) *Nature 341*, 755–757.

Siekierka, J. J., Wiederrecht, G., Greulich, H., Boulton, D., Hung, S. H. Y., Cryan, J., Hodges, P. J., & Sigal, N. H. (1990) *J. Biol. Chem. 265*, 21011–21015.

Tanford, C. (1968) *Adv. Protein Chem. 23*, 121–168.

Van Duyne, G. D., Standaert, R. F., Karplus, P. A., Schreiber, S. L., & Clardy, J. (1991) *Science 252*, 839–842.